Zoledronic acid induces cell-cycle prolongation in murine lung cancer cells by perturbing cyclin and Ras expression

Ying-Ying Li[a,b], John W-C. Chang[b], Ying-Chieh Liu[c], Cheng-Hsu Wang[a], Hsin-Ju Chang[b], Meng-Chun Tsai[d], Shiawhwa Paul Su[e] and Kun-Yun Yeh[a]

Zoledronic acid (ZOL) was shown earlier to prolong survival in animal models of lung cancer. The aim of this study was to examine whether alteration of intracellular cyclins, cyclin-dependent kinases, cyclin-dependent kinase inhibitors, retinoblastoma, and Ras protein expression and E2F localization are among the possible antilung cancer mechanisms driven by ZOL. Furthermore, we used geranylgeraniol to test whether the mevalonate pathway is involved in the antitumor effects of ZOL against lung cancer. Line-1 cells, a murine lung adenocarcinoma cell line, were examined. ZOL significantly slowed the growth of these cells both *in vitro* and *in vivo*. The ZOL-treated cells typically arrested at the S/G2/M phase of the cell cycle, accompanied by increased intracellular levels of cyclin A, B1, and CDC2 and decreased levels of cyclin D, p21, p27, phosphorylated retinoblastoma, and Ras. In addition, ZOL affected the distribution of E2F. When geranylgeraniol was added to the ZOL-treated cells, either *in vitro* or *in vivo*, tumor growth, cell-cycle progression, the expression of certain cyclins, and cyclin-related regulatory proteins were partially returned to that of untreated controls. Therefore, ZOL elicits cell-cycle prolongation that seems to be associated with alterations in the levels of certain cyclins and cyclin-related regulatory proteins. Furthermore, the mevalonate pathway regulates ZOL-induced murine lung cancer inhibition both *in vitro* and *in vivo*. *Anti-Cancer Drugs* 22:89–98 © 2011 Wolters Kluwer Health | Lippincott Williams & Wilkins.

Anti-Cancer Drugs 2011, **22**:89–98

Keywords: cell cycle, cyclins, lung cancer, Ras protein, zoledronic acid

[a]Division of Hemato-Oncology, Department of Internal Medicine, Chang Gung Memorial Hospital, Keelung & Chang Gung University, [b]Division of Hemato-Oncology, Department of Internal Medicine, Chang Gung Memorial Hospital, Kweishan & Chang Gung University, College of Medicine, [c]Department of Food Science, National Taiwan Ocean University, Keelung, [d]Yang-Ming University Instrumentation Resource Center, Taipei and [e]College of Agriculture and Natural Resources, Department of Soil & Environmental Sciences, National Chung Hsing University, Taichung, Taiwan

Correspondence to Dr Kun-Yun Yeh, Division of Hemato-Oncology, Department of Internal Medicine, Chang Gung Memorial Hospital, Keelung & Chang Gung University, College of Medicine, 222 Maijin Road, Keelung, Taiwan
Tel: +886 2 24313131 x3168; fax: +886 2 2435342;
e-mail: yehtyng@gmail.com

Received 4 June 2010 **Revised form accepted** 31 August 2010

Introduction

Zoledronic acid (ZOL), a nitrogen-containing bisphosphonate, has shown clinical benefits, such as relief from non-small cell lung cancer (NSCLC)-related bone pain and a reduction in the frequency of skeletal events associated with lung cancers, through ZOL's modulation of osetoclast activity [1,2]. ZOL inhibits the key enzymes farnesyl pyrophosphonate (FPP) synthase and geranyl–geranyl pyrophosphate (GGPP) synthase in the mevalonate (MVA) pathway, leading to interference with a variety of cellular functions essential for osteoclast survival [3,4]. Certain intermediates in the MVA pathway, such as FPP and GGPP, are required for prenylation of small GTPases such as Ras [4].

In addition, ZOL has been shown to elicit a direct antitumor effect against a variety of tumor cell lines [5–10]. By targeting enzymes such as FFP synthase and GGPP synthase, which participate in the MVA pathway and inhibit the prenylation of small GTPases, ZOL exerts its antitumor activity through inhibition of cell proliferation, induction of apoptosis, prevention of cell adhesion, and antiangiogenesis activities [5–7,10,11].

Cyclins and cyclin-dependent kinases (CDKs) are required for cell-cycle progression [12]. Different CDKs are activated at certain cell-cycle stages through association with their corresponding cyclins, which then phosphorylate regulatory proteins [including retinoblastoma (Rb) family members] and promote cell-cycle progression [12]. The G1/S transition is controlled by cyclin D, which activates CDK4 and CDK6, and subsequently by cyclin E, which associates with CDK2 [13]. The cyclin D-CDK4/6 and E-CDK2 complexes hyperphosphorylate Rb proteins that subsequently liberate E2F, a regulatory protein essential for S-phase entry [13]. There are two phosphorylation sites, Ser780 and Ser795, on the Rb protein important for cell-cycle progression [13]. During the S-phase and early G2 phase, the cyclin A-CDK2 complex phosphorylates several regulatory proteins that assist cell-cycle progression. The major function of the cyclin B1-CDC2 complex occurs during the G2/M phase to initiate mitosis [14]. Cyclin-CDK complexes are in turn regulated by CDK inhibitors (CDKIs), which generally suppress cell-cycle progression. There are two CDKI families. These include the INK4 group (p16, p15, p18, and p19), which form

0959-4973 © 2010 Wolters Kluwer Health | Lippincott Williams & Wilkins DOI: 10.1097/CAD.0b013e3283400a05

complexes with cyclin D-CDK4/6, and the Cip/Kip group (p21, p27, and p57), which are universal CDKIs and interact with various cyclins and CDKs [15].

Some studies have shown that ZOL is able to regulate the expression of certain intracellular cyclins. As a result, cell-cycle prolongation is likely and tumor growth is slowed [9,16]. In contrast, the use of geranylgeraniol (GGOH), a cell-permeable analog of the MVA intermediary GGPP, has been reported to promote protein geranylgeranylation and rescue tumor cells from the growth inhibition elicited by ZOL in certain prostate and melanoma cell lines [8,17,18].

We had shown earlier that ZOL inhibits the growth of murine lung adenocarcinomas by cell-cycle prolongation [19]. In this study, we evaluated whether ZOL could affect the expression of cell-cycle proteins, such as cyclins, CDKs, CDKIs, Rb, E2F, and Ras, that lead to tumor growth inhibition of NSCLC. We also determined if these effects occurred through the MVA pathway. We used line-1 tumor cells, a murine lung cancer cell line, to investigate the outcome of ZOL-treatment on cell growth and cell-cycle progression. The tumor behaviour of line-1 cells is similar to that of human pulmonary adenocarcinomas [20]. Finally, we used GGOH to investigate whether the MVA pathway plays a significant role in the antitumor activity of ZOL against NSCLC both *in vitro* and *in vivo*.

Materials and methods

Study animals

BALB/cByJ mice, 6–8 weeks of age, were purchased from the Taiwan National Laboratory Animal Center. Guidelines for the humane treatment of animals were followed throughout the period of animal involvement, and the treatment guidelines and experiment designs were approved by the Committee for Animal Resources at the Chang Gung Memorial Hospital and Chang Gung University, Taiwan.

Line-1 tumor cell line

Line-1 cancer cells, originally derived from BALB/cByJ mice, were initially developed by Dr John Yuhas [20] and provided by Dr Edith Lord (University of Rochester, New York, USA). This cell line was maintained in complete culture medium using RPMI 1640 (Biowest, Nuaillé, France) supplemented with 10% fetal bovine serum (Hyclone, Waltham, Massachusetts, USA), penicillin (500 units/ml), and streptomycin (200 μg/ml) (Life Technologies, Gland Island, New York, USA) in a humidified incubator at 37°C with 5% CO_2 in air.

3-(4,5-dimethylthiazol-2-yl)-2,5-diphenyltetrazolium bromide assay

A total of 1×10^4 line-1 cells were cultured in 96-well tissue-culture plates overnight and then treated with 50 μmol/l or 100 μmol/l of ZOL for one of the three different time periods (24, 48, or 72 h). ZOL (Zometa®; Novartis Pharmaceuticals, Basel, Switzerland) is hydrophilic and soluble in our selected culture medium and also in phosphate-buffered saline (PBS). The concentration of the ZOL stock was 4 mg/ml in calcium-free infusion solution (0.9% sodium-chloride solution or 5% glucose solution). In addition, GGOH (Sigma, St Louis, Missouri, USA) is soluble in 100% ethanol. The concentration of the GGOH stock was 100 mg/ml in 100% ethanol and was stored at −20°C until required. After treatment with ZOL and/or GGOH, the line-1 cells were incubated for 3 h in a volume of 100 μl of 0.1 mg/ml 3-(4,5-dimethylthiazol-2-yl)-2,5-diphenyltetrazolium bromide (MTT; Sigma). To dissolve the formazan produced during the MTT assays, the cells were resuspended in 200 μl isopropanol, and the optical density (OD) of the solution was determined using a spectrometer at an incident wavelength of 570 nm. The resultant cell viability was calculated using the formula: viability = (OD of experimental well/OD of control well) × 100%.

In-vivo tumor growth

Tumor cells (10^4) in a volume of 50 μl were injected subcutaneously into the left rear thighs of BALB/cByJ mice. For the ZOL-treated groups, we administered this drug at 1 μg/kg/week on days 7, 14, and 21 after tumor-cell inoculation. For the GGOH-treated groups, 500 μg/kg of GGOH was injected intramuscularly into the right rear thighs of the ZOL-treated, line-1 tumor-bearing mice on days 8 and 20 after tumor transplantation. For the ZOL-untreated group, we injected the test mice with a volume of PBS equal to the injected volume of ZOL in the experimental group on the above-mentioned days and anatomical locations. The largest (i) and the smallest (ii) superficial diameters of the tumors were measured every 3 days using vernier callipers. The tumor volume was calculated using the formula $V = a \times b^2/2$. The animals were killed when their leg size reached 15–16 mm in diameter.

Cell-cycle analysis

Line-1 cells were harvested after control treatment, ZOL treatment, and/or GGOH treatment. The cells were fixed with 70% ethanol and stored at −20°C for more than 1 week until required. After thawing and equilibration to room temperature, the cells were resuspended in PBS containing 0.5% Triton X-100 and 0.05% RNase, and then stained with 50 μg/ml propidium iodine (Sigma) and maintained at 4°C for a period of 30 min. Thereafter, the cell-cycle distribution of the line-1 cells was analyzed. The flow cytometer used for this study was a FACS-Calibur incorporating the Cell Quest software (BD Biosciences, Mountain View, California, USA) and WinMDI 2.8 software (Joseph Trotter, Salk Institute for Biological Studies, La Jolla, California, USA).

Western blot analysis

Line-1 cells were harvested after ZOL and/or GGOH treatment. Total cellular protein was extracted using a cell lysis and extraction kit (Sigma) containing protease and phosphatase inhibitors. Proteins were separated by 12–15% SDS-PAGE and then transferred onto nitrocellulose membranes (Millipore, Bedford, Massachusetts, USA). Nonspecific binding to membranes was blocked using 5% nonfat milk in TBST [10 mmol/l Tris-HCl, pH 7.4, 150 nmol/l NaCl, and 0.01% (v/v) Tween 20] for 1 h. The membranes were washed with TBST and then incubated with anticyclin A, cyclin B1, cyclin D, cyclin E, CDK4, p16, p21, p27, and β-actin antibodies, (rabbit antimouse IgG; Santa Cruz Biotechnology, Santa Cruz, California, USA) and anti-Rb, CDK6 (mouse antimouse IgG; Santa Cruz Biotechnology), CDC2 (mouse antimouse IgG; Chemicon, Billerica, Massachusetts, USA), CDK2 (Upstate Biotechnology, Lake Placid, New York, USA), Ras, phospho-Rb (Ser780), phospho-Rb (Ser795), and phospho-Rb (Ser087/811) (rabbit antimouse IgG; Cell Signalling Technology, Beverly, Massachusetts, USA) antibodies at 4°C overnight. After washing in TBST, the membranes were incubated with goat antirabbit or antimouse IgG (Santa Cruz Biotechnology) coupled with horseradish peroxidase at room temperature for 2 h. Finally, detection was performed using enhanced chemiluminescence substrate (Millipore).

Immunofluorescent staining

Line-1 cells (10^4 per well) were seeded in eight-well chamber slides and incubated at 37°C overnight. After ZOL and/or GGOH treatment, the cells were washed twice with PBS, fixed with 100% cold methanol, and then incubated at −20°C for over 2 h. Immunofluorescent staining was performed using primary antibodies raised against rabbit antimouse E2F antibodies and goat antirabbit-conjugated Alexa594 (Cell Signalling Technology). This was followed by incubation at 4°C overnight. After antibody incubation, the cells were washed with PBS and incubated with 2 μg/ml 4′,6-diamidino-2-phenylindole for 10 min. Finally, the slides were mounted with 90% glycerol and cover slips and then observed under a fluorescence microscope (DM2500; Leica, Wetzlar, Germany) and processed using the Case Data Manager software (Olympus, Tokyo, Japan).

Statistical analysis

All results are presented as mean ± standard deviation. Student's *t*-test was used to analyze the significance of the difference between the experimental groups. A *P* value of less than 0.05 was considered to represent a statistically significant difference between the two tested means.

Results

GGOH reverses the ZOL-induced antiproliferative effect on line-1 tumor cells *in vitro*

We used an MTT assay to investigate whether ZOL affected the proliferation of line-1 cancer cells *in vitro*. Line-1 cells were treated with 50 μmol/l or 100 μmol/l of ZOL for a given time period (24, 48, or 72 h). As shown in Fig. 1a, line-1 cell growth was inhibited by ZOL in a time-dependent and concentration-dependent manner.

To confirm whether ZOL suppressed line-1 cell growth through the MVA pathway, we added 10 μmol/l GGOH to line-1 cell cultures after ZOL treatment and found that GGOH significantly reversed the inhibitory effect of ZOL (Fig. 1a).

GGOH reverses the inhibitory effect of ZOL on line-1 cells *in vivo*

To confirm the in-vitro growth inhibition elicited by ZOL in line-1 cells, the effect of ZOL was investigated *in vivo*. As is depicted in Fig. 1b, after tumor inoculation, line-1 cells proliferated exponentially and the tumor size reached a peak volume of 230 mm^3 at around 27 days. In contrast, line-1 tumor growth in mice receiving three sequential weekly injections of ZOL (1 μg/kg/week) slowed significantly from day 12 after tumor inoculation as compared with the control mice. Furthermore, to confirm whether GGOH was able to reverse tumor inhibition driven by ZOL, we injected GGOH intramuscularly into line-1 tumor-bearing mice receiving ZOL, after ZOL administration, and then measured tumor growth. We found that the ZOL-treated line-1 tumors grew gradually after GGOH administration and displayed similar growth characteristics to line-1 tumors that had received no ZOL treatment. The above results showed that GGOH could reverse the ZOL-induced inhibitory effect on line-1 tumor growth *in vivo*, similar to cultured line-1 cells.

ZOL causes line-1 cells to arrest at the S/G2/M phase *in vitro*, and this is reversed by GGOH

To investigate the effect of ZOL on cell-cycle progression, flow cytometric analysis of DNA content was used to determine the phase distribution of line-1 cells. Line-1 cells showed a cell-cycle distribution typical to that of rapidly proliferating cells. An average of 53–69% of the cells had a 2*n* DNA content, corresponding to the G0/G1 phase of the normal cell cycle. A total of 9–17% of the cells had a 4*n* DNA content (G2/M), and 20–28% had a DNA content between 2*n* and 4*n*, corresponding to the S phase of the normal cell cycle (Fig. 2).

Line-1 cells having been treated with 50 μmol/l or 100 μmol/l of ZOL for 24, 48, or 72 h showed a time-dependent and concentration-dependent increase in the number of cells in the S/G2/M phase of the cell cycle, and this was accompanied by a reduction in the proportion of cells in the G0/G1 phase (Fig. 2). In particular, 29.6% of

Fig. 1

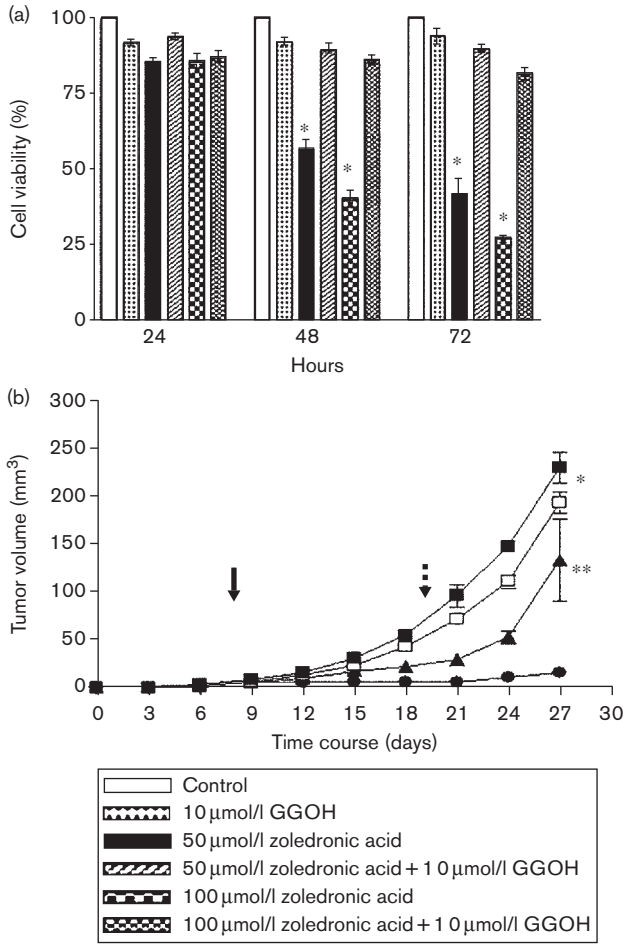

(a) Reversal of the zoledronic acid (ZOL)-induced inhibition of line-1 cell growth by geranylgeraniol (GGOH). A total of 1×10^4 line-1 cells were cultured in 96-well tissue-culture plates and treated either with or without 50 or 100 μmol/l ZOL for of the indicated time period (24, 48, or 72 h). For the GGOH experiments, 10 μmol/l GGOH was added simultaneously with ZOL to the different cultures. Cell viability was assessed by the MTT assay. Control: line-1 cells with medium alone. Data are presented as mean ± standard deviation of at least three independent experiments. *$P<0.05$ (i) between untreated and ZOL-treated cells; (ii) between ZOL-treated cells with or without addition of GGOH. (b) GGOH reversed the inhibitory effect of ZOL on tumor growth in mice. A total of 1×10^4 line-1 cells were injected subcutaneously into the left rear thighs of BALB/cByJ mice. For mice receiving ZOL treatment, we administered the drug at a rate of 1 μg/kg/week on days 7, 14, and 21 after tumor inoculation (closed circle). For mice receiving both ZOL and GGOH treatments, 500 μg/kg GGOH was injected intramuscularly into the right rear thighs of ZOL-treated line-1 tumor-bearing mice on days 8 (solid-line arrow) and 20 (dotted-line arrow) after tumor transplantation (triangle). For mice receiving GGOH treatment alone, 500 μg/kg GGOH was injected intramuscularly into the right rear thighs of untreated line-1 tumor-bearing mice on days 8 (solid-line arrow) and 20 (dotted-line arrow) after tumor transplantation (closed square). For the untreated line-1 tumor mouse group (closed square), we injected an equal volume of PBS. Each group contained five mice, the mean tumor volume ± standard deviation is presented. Three independent experiments were performed. *$P<0.05$ for mice receiving ZOL treatment compared with untreated mice. **$P<0.05$ between ZOL-treated tumor-bearing mice treated with or without GGOH.

the cells after treatment with 100 μmol/l of ZOL for 72 h were in the G0/G1 phase of the cell cycle, and those cells in the S/G2/M phase reached as high as 70.4% (Fig. 2q). Interestingly, we did not observe any apoptotic sub-G0/G1 peak for the line-1 cells after ZOL treatment.

When GGOH (10 μmol/l) was added to the line-1 cell cultures after ZOL treatment, the cell-cycle distribution nearly returned to that observed for the line-1 cells that had been treated with GGOH alone (Fig. 2). The concentration of GGOH used in this study seemed to modestly increase the proportion of cells in the S/G2/M phase in a time-dependent manner (Fig. 2). These observations suggested that ZOL caused line-1 cells to be 'trapped' in the S/G2/M phase, and that this effect required the MVA pathway.

ZOL perturbs the expression of cyclins, CDKs, and CDKIs in line-1 cells

To further characterize the effect of ZOL on cyclin expression in line-1 cells, we examined the levels of intracellular cyclins by western blot analysis. We found that a 48-h ZOL treatment increased the expression of cyclins A and B1 but decreased that of cyclin D (Fig. 3a). ZOL seemed to not affect cyclin E expression (Fig. 3a). Furthermore, a 72-h ZOL treatment showed similar patterns of cyclins A, B1, D, and E expression as seen after a 48-h treatment (data not shown).

When GGOH (10 μmol/l) was added to the line-1 cell cultures after a 48-h ZOL treatment, the intracellular expression of cyclins A, B1, and D partially returned to the levels seen in the control cultures treated with GGOH only (Fig. 3a). Furthermore, GGOH was also able to reverse the effect of a 72-h ZOL treatment on the expression of cyclins A, B1, D, and E in line 1 cells (data not shown).

We also evaluated the effect of ZOL on CDK expression by western blot analysis and observed the following after a 48-h ZOL treatment: (i) ZOL-treated line-1 cells showed increased expression of CDC2, which was partially reversed by the addition of GGOH (Fig. 3b), and (ii) ZOL seemed to not affect CDK2, CDK4, or CDK6 expression (Fig. 3b). Furthermore, line-1 cells, after a 72-h ZOL treatment, showed similar patterns of CDC, CDK2, CDK4, and CDK6 expression as those seen after a 48-h ZOL treatment (data not shown).

As ZOL altered the expression of cyclins and CDKs, we determined the expression status of CDKIs (including p16, p21, and p27), which are involved in the regulation of CDK-cyclin complexes. As depicted in Fig. 3c, ZOL treatment downregulated both p21 and p27 expression, and GGOH partially protected p21 and p27 expression from the effect of ZOL treatment. The expression of p16 was not affected by either ZOL or GGOH in line-1 cells. Taken together, these results suggested that ZOL indeed

Fig. 2

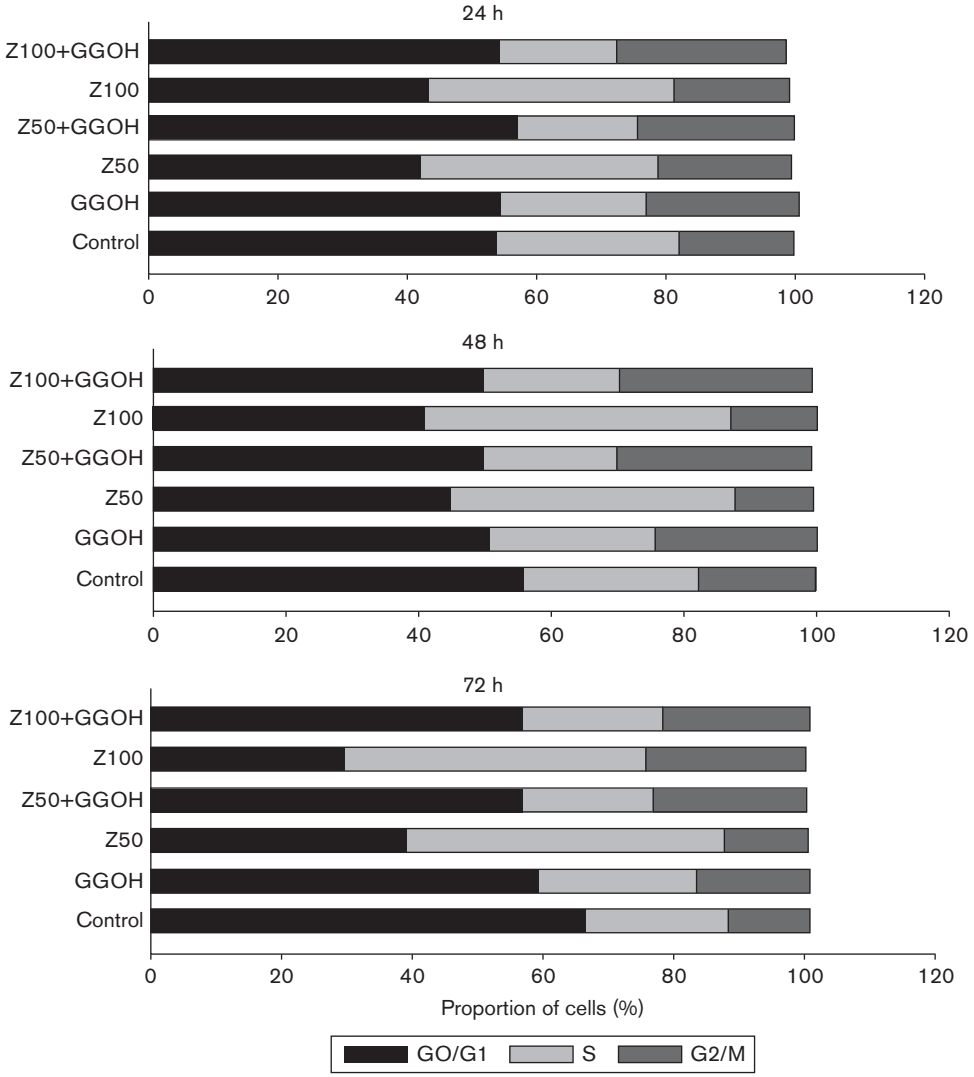

Flow cytometric analysis of DNA content for the zoledronic acid (ZOL)-treated line-1 tumor cells in the presence of geranylgeraniol (GGOH). The cells were incubated for 24, 48, or 72 h under one of the following sets of conditions: control: in culture medium alone; GGOH, in the presence of GGOH alone; Z50, in the presence of ZOL at a concentration of 50 μmol/l; Z50 + GGOH, in the presence of ZOL at a concentration of 50 μmol/l and with GGOH at a concentration of 10 μmol/l; Z100, in the presence of ZOL at a concentration of 100 μmol/l; Z100 + GGOH, in the presence of ZOL at a concentration of 100 μmol/l and with GGOH at a concentration of 10 μmol/l. The cells were harvested, fixed, and stained with propidium iodine. Three independent experiments were performed for each experiment conducted, and the proportion (percentage) of cells in each of the various stages of the cell cycle is presented from one representative experiment.

alters the expression levels of certain cyclins, CDKs, and CDKIs within line-1 cells and that the MVA pathway mediates this effect.

In-vitro effects of ZOL on Rb phosphorylation and E2F translocation

As one of the known substrates of CDKs, the extent of Rb phosphorylation is likely altered by drug modulation of CDKs [21,22]. Thus, phosphospecific antibodies to Ser780, Ser795, and Ser807/811 of Rb were used to investigate the phosphorylation status of the Rb protein in line-1 cells after a 48-h ZOL treatment. As determined by western blot analysis (Fig. 4a), we found that the ZOL-treated cells had reduced phosphorylation of Rb at Ser780, Ser795, and Ser807/811. It was also noted that Ser807/811 phosphorylation did not decrease as much as that of Ser780 or Ser795. Furthermore, treatment with ZOL seemed to not affect the overall expression of the Rb protein. When GGOH (10 μmol/l) was added to the line-1 cell cultures after a 48-h ZOL treatment, the hypophosphorylation status of Rb induced by ZOL was partially returned to the levels of the control cells treated with GGOH only. The concentration of GGOH used in this study seemed to modestly decrease the

Fig. 3

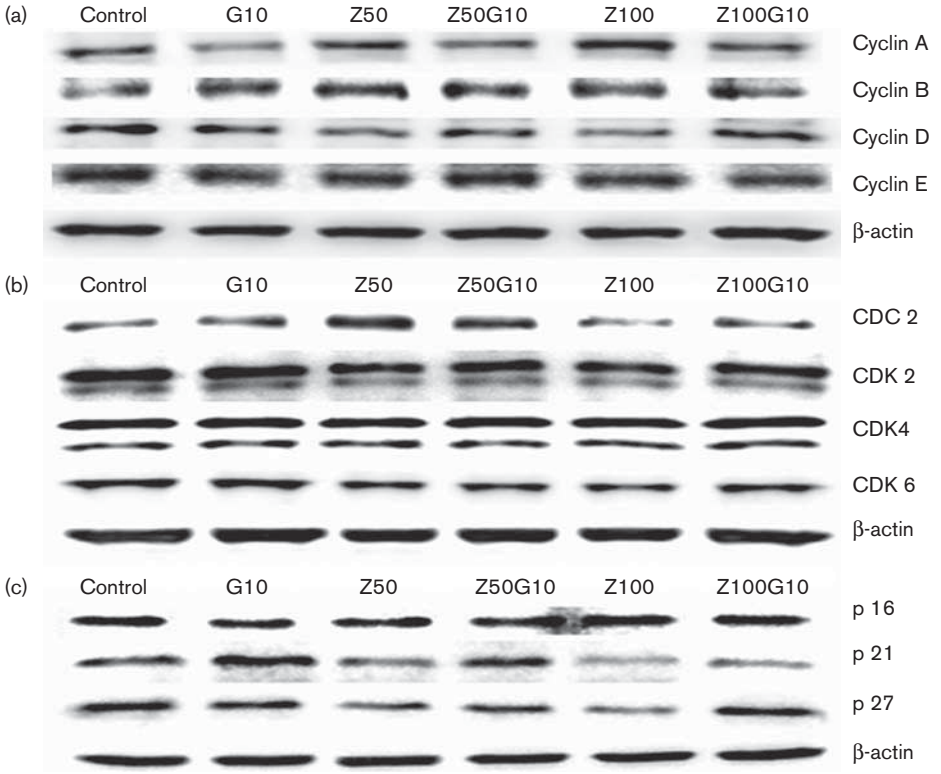

Western blot analysis depicting the effect of zoledronic acid (ZOL) on the intracellular cyclins A, B, D, and E levels (a); CDC2, cyclin-dependent kinase 2 (CDK2), CDK4, and CDK6 levels (b); and p16, p21, and p27 levels (c) in the presence of GGOH. Cells were incubated for 48 h under one of the following sets of conditions: control: culture medium alone; G10, in the presence of GGOH alone; Z50, in the presence of ZOL at a concentration of 50 μmol/l; Z50G10, in the presence of ZOL at a concentration of 50 μmol/l and with GGOH at a concentration of 10 μmol/l; Z100, in the presence of ZOL at a concentration of 100 μmol/l; Z100G10, in the presence of ZOL at a concentration of 100 μmol/l and with GGOH at a concentration of 10 μmol/l.

Fig. 4

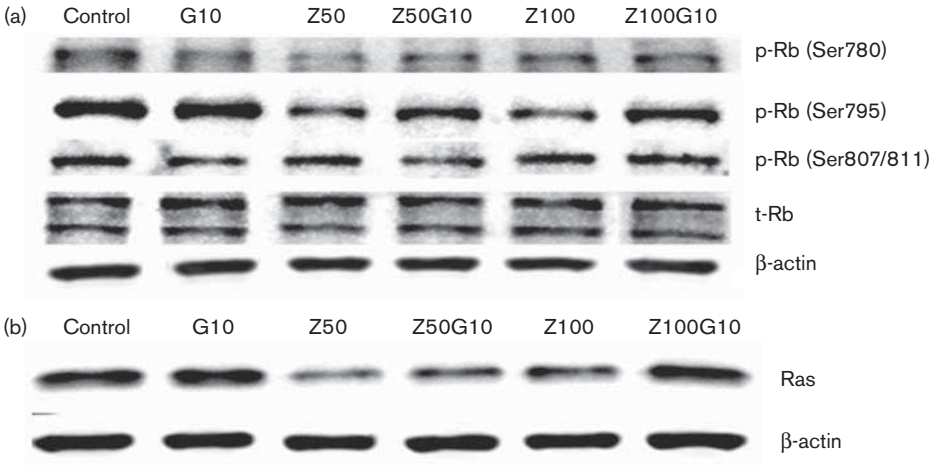

Western blot analysis depicting the effect of zoledronic acid (ZOL) on the phosphorylation of the retinoblastoma (Rb) protein (a) and Ras protein (b) levels in the presence of geranylgeraniol (GGOH). Cells were incubated for 48 h under one of the following sets of conditions: control: in culture medium alone; G10, in the presence of GGOH alone; Z50, in the presence of ZOL at a concentration of 50 μmol/l; Z50G10, in the presence of ZOL at a concentration of 50 μmol/l and with GGOH at a concentration of 10 μmol/l; Z100, in the presence of ZOL at a concentration of 100 μmol/l; Z100G10, in the presence of ZOL at a concentration of 100 μmol/l and with GGOH at a concentration of 10 μmol/l.

Fig. 5

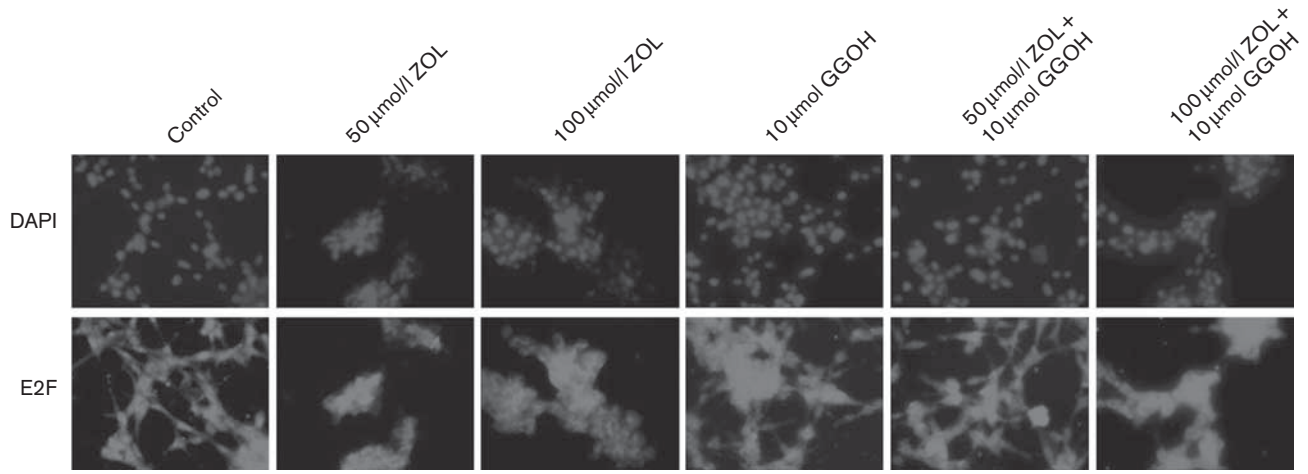

Zoledronic acid (ZOL) affects E2F translocation from the cytoplasm to the nuclei in line-1 tumor cells. Cells were treated with the same conditions as those described in Fig. 4 and then stained with E2F antibodies. Nuclei were visualized by 4′,6-diamidino-2-phenylindole (DAPI) staining. Magnification, × 400. GGOH, geranylgeraniol.

phosphorylation of the Rb protein. These observations suggested that ZOL induced the hypophosphorylation of Rb through the MVA pathway, and this might be involved in the observed cell-cycle prolongation in line-1 cells.

To examine whether Rb hypophosphorylation affected E2F translocation from the cytoplasm to the nucleus, we used immunofluorescent staining to determine the position of E2F. As shown in Fig. 5, E2F expression could be seen most prominently in the nuclei (relative to the cytoplasm) in the cells treated with the culture medium alone or GGOH (10 μmol/l). In contrast, condensed E2F was detected in the cytoplasm surrounding the nuclei in the presence of ZOL. In the cells treated with both GGOH and ZOL, E2F distribution was similar to that of the control groups. This observation suggested that E2F was retained in the cytoplasm after ZOL treatment, and that this was reversed by the addition of GGOH.

ZOL downregulates the level of Ras expression in line-1 cells

Matsumoto *et al.* [23] reported that ZOL is able to inhibit the prenylation of Ras proteins, resulting in the inhibition of the growth of small cell lung cancer cells. Tassone *et al.* [7], in contrast, observed that ZOL elicited a reduction in the intracellular Ras levels. Thus, we evaluated whether ZOL affected the prenylation process or intracellular expression of Ras in line-1 cells. We did not detect any change in the Ras expression in line-1 cells up to 48 h of ZOL treatment. The intracellular level of Ras was noted to decline as compared with the controls after 48 h of ZOL treatment (Fig. 4b), and the extent of this decline was also consistently noted when the line-1 cells were treated with ZOL over a 72-h period (data not shown). When GGOH (10 μmol/l) was added to the ZOL-treated line-1 cell cultures, the expression of the Ras proteins partially returned to that of the line-1 cells receiving no ZOL treatment. Interestingly, we did not detect any prenylated form of Ras at any of the timepoints (24, 48, or 72 h).

Discussion

The mechanisms underpinning the prolongation of the cell cycle in line-1 cells induced by ZOL could be related to the alterations to the intracellular levels of certain cyclins. Kuroda *et al.* [16] reported that ZOL was able to impair expression of certain cell cycle-dependent cyclins such as cyclins A, B, and D3 in the BV173 leukemia cell line. Another study, conducted by Kubista *et al.* [9], showed that ZOL induced cells accumulate in the S-phase accompanied by a prominent loss of intracellular cyclins D1 and E in a prostate-cancer cell line. For the line-1 tumor cell model investigated in this study, ZOL administration resulted in decreased levels of G1/S-phase cyclin D expression and increased levels of S-phase cyclin A and G2/M-phase cyclin B1 expression, and no change in cyclin E expression. Furthermore, the increased level of expression among CDKs in the ZOL-treated line-1 cells was only observed for CDC2, which is essential at the G2/M phase of cell-cycle progression. Taken together, this study showed that the increased levels of S/G2/M-associated cyclins and CDKs-cyclin A, cyclin B1, and CDC2 may lead to the ZOL-driven cell-cycle arrest at the S/G2/M phase in NSCLC cells.

An important target of the cyclin D–CDK4/6 complex during the G1-to-S transition is Rb, which regulates cell proliferation and differentiation [24]. While cells are in

the G1-to-S transition, Ras modulates cyclin D expression through the ERK pathway and further affects Rb phosphorylation (at Ser780, Ser795, and Ser807/811) and E2F translocation. Our results showed that Rb was hypophosphorylated and E2F translocation to the nuclei was restrained, possibly because of the lower expression of cyclin D in cells after ZOL treatment [25,26]. In contrast, hypophosphorylation of Rb acts as an inhibitor of the G1-to-S transition [27], and agents that induce hypophosphorylation of Rb can lead to G1 cell-cycle arrest [28–30]. Paradoxically, this study showed that phosphorylation of the Rb protein was decreased, but the cell cycle was arrested at the S/G2/M phase in the line-1 cells after ZOL treatment. This discrepancy could, in part, be explained as follows: first, earlier reports have indicated that although CDKs are constitutively expressed, the change in expression of cyclins is critical at certain stages of cell-cycle progression [28,31]. The decreased level of cyclin D expression detected in this study may have led to the reduction of phosphorylation of Rb. Second, Zhang *et al.* [14] reported that there is decreased phosphorylation of Rb at Ser795, but an increased percentage of G2/M-phase cells in HCT116 colorectal cancer cells after application of a pan-CDK inhibitor, AG-012986, at 240 nmol/l for over 24 h. The simultaneous occurrence of Rb hypophosphorylation and G2/M-phase arrest under certain circumstances is possible. Finally, cell-cycle progression in line-1 cells after ZOL treatment became less mitotic and arrested at the S/G2/M phase. Thus, the G1-to-S transition stage in the cell cycle turned out to be less active, and the detection of the presence of the hypophosphorylation status of Rb in the ZOL-treated line-1 tumor cells is reasonable.

A critical role for Ras in cell-cycle progression has been shown by both the microinjection of neutralizing antiRas antibodies and by the expression of dominant interfering Ras [32]. Cyclin D is an important target of the mitogenic Ras signalling cascade [33,34]. In addition, it has been shown that Ras promotes p21 and p27 expression, which downregulates and captures cyclins D and A, and subsequently causes dissociation of the cyclin–CDK complexes during the G1-to-S phase [35–37]. Hence, decreased Ras levels caused by ZOL treatment may lead to a decline in the p21 and p27 protein levels but enhancement in the level of cyclin A expression in line-1 tumor cells.

GGOH, which can be exogenously taken up by cells and controverted to GGPP as a salvage pathway subsequent to the blockade of the MVA pathway, would seem to be more active with regard to its ability to antagonize the anticancer activity of ZOL compared with the impact of other analogs of the MVA pathway, such as FOH [17]. GGOH has been reported earlier to inhibit ZOL-induced apoptosis in breast and prostate cancer cells [38]. In addition, GGOH has been noted to prevent the arrest of normal cell-cycle progression and the inhibition of cell proliferation induced by either bisphosphonate incadronate or mevastain more robustly than FOH [11]. The investigators of another related study documented that exogenous GGOH, but not FOH, was able to overcome the blockade to tyrosine phosphorylation of the platelet-derived growth-factor receptors imposed by lovastin [39]. Denoyelle *et al.* [40] showed that the microfilament activity of ZOL was blocked by GGOH, but not by FOH, in breast cancer cells. Although Ras is an example of a primary farnesylated protein, an alternative pattern of prenylation has been noted to occur in K-Ras for cases of FPP deficiency [17]. Furthermore, for certain osteosarcoma cell lines, the level of inactivation of Rap1, a geranylgeranylated GTPase, correlated well with the relative sensitivity of these cancer cells toward ZOL-mediated cytotoxicity [9]. We performed the western blot analysis for the in-vivo prenylation status of line-1 tumor cells treated with ZOL. We found that ZOL inhibited Rap-1a prenylation, but this inhibitory effect could be partially reverse by GGOH *in vivo* (data not shown). Taken together, such results suggest that the MVA requirement relating to ZOL-driven anticancer activity may not be satisfied by simply restoring protein farnesylation, but may involve incorporating a certain level of protein geranylgeranylation.The most puzzling part of analyzing the so-called in-vivo antitumor effect of ZOL in this study is the dose discrepancy between the in-vitro and in-vivo conditions. First, ZOL is rapidly cleared from circulation according to pharmacokinetics. A peak serum concentration of ZOL after administration ranging from 1 to 5 μmol/l is maintained for a few hours after a 4 mg ZOL dose, which is the recommended dosage for cancer-related skeletal disorders [41]. Most of the administered dose binds to the skeleton and tissues characterized by the high turnover rate [42,43]. It is possible that ZOL accumulates within the tumor microenvironment where it reaches a relatively high concentration, even though a low dose of ZOL is administered. The dose used in the in-vitro study is a short-term observation that offers a useful way to delineate possible underlying mechanisms, but it might not be well extrapolated to a long-term in-vivo observation under some circumstances. Furthermore, we believe that in addition to the direct tumor inhibitory effect, certain other effects generated by ZOL, including cell-cycle prolongation, inhibition of angiogenesis, and prevention of cancer cell adhesion and invasion, are important for ZOL's antitumor activity. The required concentration of ZOL to block prostate cancer invasion and adhesion ranges from 10^{-12} to 10^{-6} M only [44,45]. Matsumoto *et al.* [23] used a low dose of ZOL and showed the inhibition of small cell lung cancer growth in an animal model. We showed earlier that a low dose of ZOL is able to elicit cell cycle prolongation in NSCLC *in vivo* [19]. Therefore, it may not be necessary for the dose of ZOL used in the tested animal to be as high as the in-vitro concentration.

The somewhat limited solubility of GGOH in aqueous solution has been shown to result in a significant amount of the added GGOH to be embedded into the cellular membrane, thus generating injury that could be detrimental to cell growth [17]. Fortunately, this difficulty was overcome in our experiments by the serial titration of GGOH with the organic solvent ethanol. We found that GGOH could be completely dissolved in 0.5% ethyl alcohol, at which point either GGOH or ethyl alcohol alone was unable to induce line-1 cell death (data not shown). This breakthrough led us to manipulate GGOH administration both *in vitro* and *in vivo* and allowed us to complete an original experiment using GGOH to reverse the ZOL-driven anticancer activity *in vivo*. Consequently, we confirmed that the MVA pathway is indeed involved in the ZOL-induced NSCLC-elicited tumor-growth/tumor-cell growth inhibition.

In conclusion, using a murine lung adenocarcinoma cell line, we have clearly shown that cell-cycle prolongation driven by ZOL is associated with an alteration in the intracellular expression of certain cyclins, CDC2, p21, p27, and Ras. Using GGOH, this study has provided the first evidence that the MVA pathway indeed regulates the ZOL-induced cell-cycle prolongation and NSCLC growth inhibition both *in vitro* and *in vivo*. We propose that ZOL may be a useful and novel therapeutic option for the treatment of human lung cancer patients in the near future.

Acknowledgements

This study was supported by a Grant (NMRPG330062) from the National Science Council and a Grant (CMRPG350381) from the Chung Gang Memorial Hospital.

There is no conflict of interest to declare in employment (other than primary affiliations), commercial grant, other commercial research support, ownership interest, consultant/advisory board and honoraria from speakers' bureau.

References

1 Rosen LS, Gordon D, Tchekmedyian S, Yanagihara R, Hirsh V, Krzakowski M, *et al.* Zoledronic acid versus placebo in the treatment of skeletal metastases in patients with lung cancer and other solid tumors: a phase III, double-blind, randomized trial – the Zoledronic Acid Lung Cancer and Other Solid Tumors Study Group. *J Clin Oncol* 2003; **21**:3150–3157.

2 Saba N, Khuri F. The role of bisphosphonates in the management of advanced cancer with a focus on non-small-cell lung cancer. Part 1: mechanisms of action, role of biomarkers and preclinical applications. *Oncology* 2005; **68**:10–17.

3 Rogers MJ, Frith JC, Luckman SP, Coxon FP, Benford HL, Monkkonen J, *et al.* Molecular mechanisms of action of bisphosphonates. *Bone* 1999; **24** (**5 Suppl**):73S–79S.

4 Luckman SP, Hughes DE, Coxon FP, Graham R, Russell G, Rogers MJ. Nitrogen-containing bisphosphonates inhibit the mevalonate pathway and prevent post-translational prenylation of GTP-binding proteins, including Ras. *J Bone Miner Res* 1998; **13**:581–589.

5 Fromigue O, Lagneaux L, Body JJ. Bisphosphonates induce breast cancer cell death *in vitro*. *J Bone Miner Res* 2000; **15**:2211–2221.

6 Hiraga T, Williams PJ, Ueda A, Tamura D, Yoneda T. Zoledronic acid inhibits visceral metastases in the 4T1/luc mouse breast cancer model. *Clin Cancer Res* 2004; **10**:4559–4567.

7 Tassone P, Tagliaferri P, Viscomi C, Palmieri C, Caraglia M, D'Alessandro A, *et al.* Zoledronic acid induces antiproliferative and apoptotic effects in human pancreatic cancer cells *in vitro*. *Br J Cancer* 2003; **88**:1971–1978.

8 Forsea AM, Muller C, Riebeling C, Orfanos CE, Geilen CC. Nitrogen-containing bisphosphonates inhibit cell cycle progression in human melanoma cells. *Br J Cancer* 2004; **91**:803–810.

9 Kubista B, Trieb K, Sevelda F, Toma C, Arrich F, Heffeter P, *et al.* Anticancer effects of zoledronic acid against human osteosarcoma cells. *J Orthop Res* 2006; **24**:1145–1152.

10 Ory B, Heymann MF, Kamijo A, Gouin F, Heymann D, Redini F. Zoledronic acid suppresses lung metastases and prolongs overall survival of osteosarcoma-bearing mice. *Cancer* 2005; **104**:2522–2529.

11 Jagdev SP, Coleman RE, Shipman CM, Rostami HA, Croucher PI. The bisphosphonate, zoledronic acid, induces apoptosis of breast cancer cells: evidence for synergy with paclitaxel. *Br J Cancer* 2001; **84**:1126–1134.

12 Howard CM, Claudio PP, De Luca A, Stiegler P, Jori FP, Safdar NM, *et al.* Inducible pRb2/p130 expression and growth-suppressive mechanisms: evidence of a pRb2/p130, p27Kip1, and cyclin E negative feedback regulatory loop. *Cancer Res* 2000; **60**:2737–2744.

13 Sherr CJ, Roberts JM. CDK inhibitors: positive and negative regulators of G1-phase progression. *Genes Dev* 1999; **13**:1501–1512.

14 Zhang C, Lundgren K, Yan Z, Arango ME, Price S, Huber A, *et al.* Pharmacologic properties of AG-012986, a pan-cyclin-dependent kinase inhibitor with antitumor efficacy. *Mol Cancer Ther* 2008; **7**:818–828.

15 Lloyd RV, Erickson LA, Jin L, Kulig E, Qian X, Cheville JC, *et al.* p27kip1: a multifunctional cyclin-dependent kinase inhibitor with prognostic significance in human cancers. *Am J Pathol* 1999; **154**:313–323.

16 Kuroda J, Kimura S, Segawa H, Sato K, Matsumoto S, Nogawa M, *et al.* p53-independent anti-tumor effects of the nitrogen-containing bisphosphonate zoledronic acid. *Cancer Sci* 2004; **95**:186–192.

17 Crick DC, Andres DA, Waechter CJ. Novel salvage pathway utilizing farnesol and geranylgeraniol for protein isoprenylation. *Biochem Biophys Res Commun.* 1997; **237**:483–487.

18 Goffinet M, Thoulouzan M, Pradines A, Lajoie-Mazenc I, Weinbaum C, Faye JC, *et al.* Zoledronic acid treatment impairs protein geranyl-geranylation for biological effects in prostatic cells. *BMC Cancer* 2006; **6**:60. [Electronic resource]

19 Li YY, Chang JW, Chou WC, Liaw CC, Wang HM, Huang JS, *et al.* Zoledronic acid is unable to induce apoptosis, but slows tumor growth and prolongs survival for non-small-cell lung cancers. *Lung Cancer* 2008; **59**:180–191.

20 Yuhas JM, Pazmino NH. Inhibition of subcutaneously growing line 1 carcinomas due to metastatic spread. *Cancer Res* 1974; **34**:2005–2010.

21 Boulikas T. Phosphorylation of transcription factors and control of the cell cycle. *Crit Rev Eukaryot Gene Expr* 1995; **5**:1–77.

22 Lundberg AS, Weinberg RA. Functional inactivation of the retinoblastoma protein requires sequential modification by at least two distinct cyclin-cdk complexes. *Mol Cell Biol* 1998; **18**:753–761.

23 Matsumoto S, Kimura S, Segawa H, Kuroda J, Yuasa T, Sato K, *et al.* Efficacy of the third-generation bisphosphonate, zoledronic acid alone and combined with anti-cancer agents against small cell lung cancer cell lines. *Lung Cancer* 2005; **47**:31–39.

24 Weinberg RA. The retinoblastoma protein and cell cycle control. *Cell* 1995; **81**:323–330.

25 Xiong W, Pestell RG, Watanabe G, Li J, Rosner MR, Hershenson MB. Cyclin D1 is required for S phase traversal in bovine tracheal myocytes. *Am J Physiol* 1997; **272** (6 Pt 1):L1205–L1210.

26 Ramakrishnan M, Musa NL, Li J, Liu PT, Pestell RG, Hershenson MB. Catalytic activation of extracellular signal-regulated kinases induces cyclin D1 expression in primary tracheal myocytes. *Am J Respir Cell Mol Biol* 1998; **18**:736–740.

27 Ezhevsky SA, Nagahara H, Vocero-Akbani AM, Gius DR, Wei MC, Dowdy SF. Hypo-phosphorylation of the retinoblastoma protein (pRb) by cyclin D: Cdk4/6 complexes results in active pRb. *Proc Natl Acad Sci U S A* 1997; **94**:10699–10704.

28 Hosako M, Ogino T, Omori M, Okada S. Cell cycle arrest by monochloramine through the oxidation of retinoblastoma protein. *Free Radic Biol Med* 2004; **36**:112–122.

29 Tyagi A, Agarwal C, Agarwal R. Inhibition of retinoblastoma protein (Rb) phosphorylation at serine sites and an increase in Rb-E2F complex formation

by silibinin in androgen-dependent human prostate carcinoma LNCaP cells: role in prostate cancer prevention. *Mol Cancer Ther* 2002; **1**:525–532.
30 Dimberg A, Bahram F, Karlberg I, Larsson LG, Nilsson K, Oberg F. Retinoic acid-induced cell cycle arrest of human myeloid cell lines is associated with sequential down-regulation of c-Myc and cyclin E and posttranscriptional up-regulation of p27(Kip1). *Blood* 2002; **99**:2199–2206.
31 Shackelford RE, Kaufmann WK, Paules RS. Oxidative stress and cell cycle checkpoint function. *Free Radic Biol Med* 2000; **28**:1387–1404.
32 Mulcahy LS, Smith MR, Stacey DW. Requirement for ras proto-oncogene function during serum-stimulated growth of NIH 3T3 cells. *Nature* 1985; **313**:241–243.
33 Mittnacht S, Paterson H, Olson MF, Marshall CJ. Ras signalling is required for inactivation of the tumour suppressor pRb cell-cycle control protein. *Curr Biol* 1997; **7**:219–221.
34 Peeper DS, Upton TM, Ladha MH, Neuman E, Zalvide J, Bernards R, *et al.* Ras signalling linked to the cell-cycle machinery by the retinoblastoma protein. *Nature* 1997; **386**:177–181.
35 Woods D, Parry D, Cherwinski H, Bosch E, Lees E, McMahon M. Raf-induced proliferation or cell cycle arrest is determined by the level of Raf activity with arrest mediated by p21Cip1. *Mol Cell Biol* 1997; **17**:5598–5611.
36 Kawada M, Kuwahara A, Nishikiori T, Mizuno S, Uehara Y. NA22598, a novel antitumor compound, reduces cyclin D1 levels, arrests cell cycle at G1 phase, and inhibits anchorage-independent growth of human tumor cells. *Exp Cell Res* 1999; **249**:240–247.
37 Michalides RJ, Van de Brekel M, Balm F. Defects in G1-S cell cycle control in head and neck cancer: a review. *Head Neck* 2002; **24**:694–704.
38 Neville-Webbe HL, Rostami-Hodjegan A, Evans CA, Coleman RE, Holen I. Sequence- and schedule-dependent enhancement of zoledronic acid induced apoptosis by doxorubicin in breast and prostate cancer cells. *Int J Cancer* 2005; **113**:364–371.
39 McGuire TF, Qian Y, Vogt A, Hamilton AD, Sebti SM. Platelet-derived growth factor receptor tyrosine phosphorylation requires protein geranylgeranylation but not farnesylation. *J Biol Chem* 1996; **271**:27402–27407.
40 Denoyelle C, Hong L, Vannier JP, Soria J, Soria C. New insights into the actions of bisphosphonate zoledronic acid in breast cancer cells by dual RhoA-dependent and -independent effects. *Br J Cancer* 2003; **88**:1631–1640.
41 Berenson J, Ravera C, Ma P, Deckert F, Sasaki Y, Saeki T, *et al.* Population pharmacokinetics (PK) of Zometa. *Proc Am Soc Clin Oncol* 2000; **19**:209a. (abstr 814)
42 Papapoulos SE. Bisphosphonates: how do they work? *Best Prac Res* 2008; **22**:831–847.
43 Losada I, Sartori L, Di Gianantonio E, Zen M, Clementi M, Doria A. Bisphosphonates in patients with autoimmune rheumatic diseases: can they be used in women of childbearing age? *Autoimmun Rev* 2010; **9**:547–552.
44 Boissier S, Magnetto S, Frappart L, Cuzin B, Ebetino FH, Delmas PD, *et al.* Bisphosphonates inhibit prostate and breast carcinoma cell adhesion to unmineralized and mineralized bone extracellular matrices. *Cancer Res* 1997; **57**:3890–3894.
45 Virtanen SS, Vaananen HK, Harkonen PL, Lakkakorpi PT. Alendronate inhibits invasion of PC-3 prostate cancer cells by affecting the mevalonate pathway. *Cancer Res* 2002; **62**:2708–2714.